

Effect of Target Polarization in Electron-Ion Recombination

A. V. Korol*

Department of Physics, St. Petersburg State Maritime Technical University, St. Petersburg 198262, Russia

G. F. Gribakin[†] and F. J. Currell[‡]

School of Mathematics and Physics, Queen's University, Belfast BT7 1NN, Northern Ireland, United Kingdom

(Received 27 July 2006; published 27 November 2006)

We present results of a study of the effect of target polarization on electron-ion recombination, and show that coherent radiation by the target electrons gives a large contribution to the recombination rate. It significantly modifies the nonresonant photorecombination background. A procedure has been devised whereby this contribution can be evaluated together with the conventional radiative recombination, independently of the dielectronic recombination component. Numerical results are presented for Zn^{2+} , Cd^{2+} , Sn^{4+} , and Xe^{8+} , showing up to an order-of-magnitude enhancement.

DOI: 10.1103/PhysRevLett.97.223201

PACS numbers: 34.80.Lx, 52.20.-j

Electron-ion photorecombination is usually analyzed in terms of two mechanisms, i.e., radiative recombination (RR) and dielectronic recombination (DR). The RR contribution has a smooth energy dependence and is maximal at low electron energies. DR has a characteristic resonant character, with peaks at the energies of doubly excited states of the compound ion [1]. In this Letter we show that the effect of coherent radiation of the target electron cloud polarized by the incident electron, can strongly modify the nonresonant background.

Theoretically, a complete description of the recombination process must account for all contributions (see, e.g., [2–4]). In practice one can only include a finite number of target and compound ion states, electron orbitals, and configurations. In simple systems such sets can be made practically complete. For many ions accurate recombination cross sections and rates are obtained by adding the RR and DR contributions, the latter in the independent resonance approximation (see, e.g., [5,6]). There are other cases where interference between DR resonances and RR background has been predicted [7–9] and observed [10,11].

Providing an accurate description for more complex systems with many-electron (and possibly, open) valence shells is a difficult task. Thus, state-of-the-art theoretical methods have so far failed to describe the recombination rates for Ar-like Sc^{2+} [10]. The problem here lies in the strong configuration interaction between many doubly excited states in the presence of an open $3p$ shell. In even more complex systems, like U^{28+} or Au^{25+} , the recombination rates exceed the RR rates by 2 orders of magnitude [12,13]. This is caused by extremely strong configuration mixing which involves multiply excited states. It drives the system towards the regime of many-body quantum chaos where one can use statistical methods [14–16] akin to those applied to transition arrays [17].

In this work we focus on a different recombination mechanism, i.e., *polarization recombination* (PR), in which the photon is emitted by the target ion polarized

by the incident electron [18–20]. It is known that radiation due to target polarization is an important component of the photon spectra in electron and proton bremsstrahlung on many-electron atoms and in collisional radiative processes involving clusters and fullerenes (see [21,22] and references therein). Its effect is especially prominent in the frequency ranges of giant dipole resonances which characterize many such targets. Experimental evidence for such structures in the x-ray spectra in electron collisions is reviewed in Ref. [23]. In what follows we will explain that the contribution of PR is distinct from both RR and DR. We will also show that target excitations in the continuum, which are often neglected in DR calculations, can play a prominent role in PR, increasing the RR-like background by up to an order of magnitude.

The amplitudes of RR and DR are shown schematically in Fig. 1 by diagrams (a) and (b). In RR, the incident electron with energy ε is captured into a discrete final state f , emitting a photon of energy $\omega = \varepsilon - \varepsilon_f$. In DR, the electron is captured into a doubly excited resonant state at $\varepsilon \approx \varepsilon_a + \varepsilon_b - \varepsilon_n$, which stabilizes by photoemission. Of course, the photon can also be emitted by the other electron, b , and exchange diagrams should be added. Also, to obtain correct DR resonance energies and widths, configu-

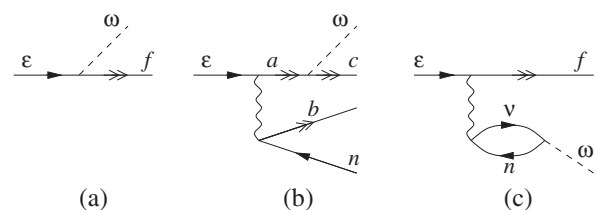


FIG. 1. Diagrammatic representation of RR (a), DR (b), and PR (c). Note that (c) includes part of DR which interferes with RR, while (b) is the noninterfering part of DR. Lines with double arrows are discrete electron states in the field of the ion, lines with the arrows to the left are holes in the target ground state, the dashed line is the photon, and the wavy line is the electron Coulomb interaction.

ration mixing between doubly excited states must be taken into account.

The PR diagram Fig. 1(c) describes a process where the photon is emitted by the target ion polarized by the incident electron. Its amplitude contains a sum over the holes n and excited electron states ν , including the continuum. Its final state is identical to that of RR diagram (a), hence the two amplitudes interfere. The contribution of discrete excited states to the sum over ν in diagram (c) accounts for a part of DR and its interference with RR. As described below, the former can be subtracted out, while preserving the contribution of the excited state continuum and interference effects.

At first glance it may appear that (c) is only a small correction to (a), since the acceleration of the target electrons due to the incident electron is much smaller than that of the incident electron in the field of the ion. However, in (c) the contributions of *all* electrons in the valence or inner shell are added *coherently* in the amplitude. The contribution of a particular target orbital nl to the PR amplitude is thus proportional to the number of electrons, N_{nl} , in this orbital.

For a qualitative estimate of PR, consider the sum of amplitudes (a) and (c),

$$\langle f|\mathbf{r}|\varepsilon\rangle + \sum_{n,\nu} \left[\frac{\langle n|\mathbf{r}|\nu\rangle\langle f\nu|V|n\varepsilon\rangle}{\omega - \omega_{\nu n} + i0} + \frac{\langle \nu|\mathbf{r}|n\rangle\langle fn|V|\nu\varepsilon\rangle}{-\omega - \omega_{\nu n} + i0} \right], \quad (1)$$

where $\omega_{\nu n} = \varepsilon_{\nu} - \varepsilon_n$, and \mathbf{r} is the dipole operator (atomic units are used). Note that a 2nd PR contribution obtained from (c) by switching the order of the Coulomb and photon interactions, has been added [20,24].

For incident electron energies smaller than the target ionization potential, and high-lying (Rydberg) final states f , amplitude (1) can be estimated as [19,20]

$$\langle f|\mathbf{r}|\varepsilon\rangle [1 - (\omega^2/Z_i)\alpha_d(\omega)], \quad (2)$$

where $\alpha_d(\omega)$ is the target dynamic dipole polarizability and Z_i is the (effective) charge of the ion. As shown in Ref. [20], Eq. (2) can lead to substantial errors when used outside its limits. However, it is still useful for a qualitative physical analysis, since it shows how PR modifies the basic RR amplitude. Depending on the value of the factor in brackets in Eq. (2), PR can either increase or reduce the recombination rate. In particular, if the target photoabsorption cross section, $\sigma_{\text{ph}}(\omega) = (4\pi\omega/c) \text{Im}\alpha_d(\omega)$, possesses a giant resonance at some energy, the recombination transitions near this energy can be strongly enhanced.

As shown in Ref. [20], the applicability of Eq. (2) to electron recombination is limited to low incident electron energies and high Rydberg final states. Hence, the estimates presented in Ref. [19], grossly exaggerated the effect. Realistic numerical calculations based on Eq. (1) demonstrated that for Ne-like and Ni-like ions with charges between +8 and +44, PR increases the recombination rates by 5%–30% in nonresonant energy intervals [20], due to constructive interference of PR and RR. In this

Letter we consider a number of ions in which the manifestation of PR is even stronger. We suggest how to separate this effect from the standard DR contribution, and show how PR modifies thermal RR recombination rates over a broad range of temperatures.

The cross section for photorecombination into the final electron state f is proportional to the squared modulus of amplitude (1). The latter was calculated by expanding the wave function of the incident electron in partial waves (see Ref. [20] for details). The electron radial wave functions were computed in the Hartree-Fock field of the target ion. Excited electron states ν (both discrete and continuous) take into account the field of the hole n , and the two are coupled into the 1P term (dipole excitations). Excitations from all orbitals with principal quantum numbers greater than one were included. The sets of final states include all principal quantum numbers up to ten. Contributions of higher Rydberg states, which are important at low projectile energies, were added to the recombination rates by using the Kramers formula.

Figure 2 compares the cross section calculated in this manner for $\text{Zn}^{2+} 3d^{10}$ using the total amplitude (1), with the RR cross section for which only the first term in Eq. (1) is retained. As explained above, the PR amplitude contains some contribution of the DR resonances, which is clearly visible in the figure. However, the effect that we want to focus on is the dramatic change of the background. For example, in the energy range between 40 and 75 eV, which contains no DR resonances, the inclusion of the PR amplitude has doubled the cross section.

We have also performed a calculation in which only discrete excited states ν are included in the PR sums in Eq. (1). The resulting cross section (thin curve in Fig. 2) still shows resonant DR peaks, but the background is now simply given by the RR cross section. This means that most of the strength of the PR amplitude comes from the target excitations into the continuum. We have checked that the

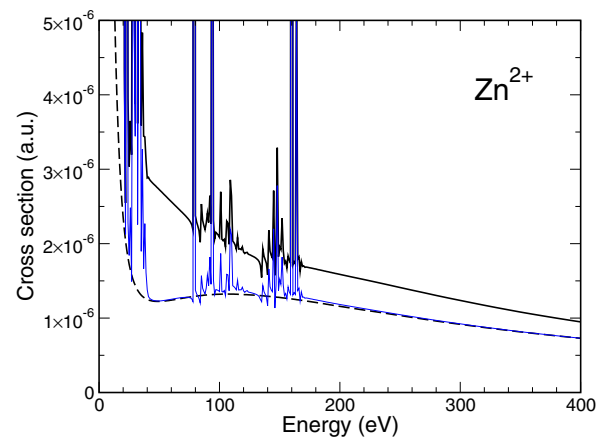


FIG. 2 (color online). Recombination cross sections for Zn^{2+} , obtained from the full RR + PR amplitude (1) (thick solid curve), with discrete target excitations in PR terms only (thin solid curve), and in the RR approximation (dashed curve).

large role of the target continuum can also be seen in the $3d$ photoionization cross section. It forms a broad maximum with $\sigma_{\text{ph}} \approx 8 \text{ Mb}$ at $\omega \approx 70 \text{ eV}$, due to the $3d \rightarrow \varepsilon f$ transition.

The results for Zn^{2+} in Fig. 2 demonstrate that a calculation performed by adding the DR resonances to the RR background, would considerably underestimate the cross section. The main effect of PR is the change of the non-resonant background. We thus want to devise a method that would account for this effect without including the resonant DR part contained in the PR. (The DR resonances can be added afterwards in the usual way.)

To implement this idea, we performed calculations using the full RR + PR amplitude (1), but omitting the squared moduli of all discrete excitation terms from the cross section. Such calculation preserves all interference and continuum contributions. For convenience, we also introduced a small width Γ (e.g., $\Gamma = 1 \text{ eV}$) in the resonant denominators. After this, the interference profiles due to discrete target excitations, whose energy dependence is given by $(\omega - \omega_{\nu n})/[(\omega - \omega_{\nu n})^2 + \Gamma^2/4]$, become finite. For small Γ this procedure does not affect the integral contribution of the interference terms.

The RR + PR cross section for Zn^{2+} with the resonances taken out, is shown in Fig. 3 by the thick solid

curve. Because of the interference, the inclusion of PR does not always increase the cross sections [25]. Qualitatively, this can be understood from Eq. (2). For ω below the characteristic dipole excitation energy of a subshell, ω_{nl} , its contribution to $\alpha_d(\omega)$ is positive. Hence, PR may suppress the recombination amplitude at energies below the DR range of the corresponding subshell (e.g., at $\varepsilon < 20 \text{ eV}$ for the $3d$ orbital in Zn^{2+}). For $\omega > \omega_{nl}$ the contribution of the subshell to the real part of $\alpha_d(\omega)$ is negative ($\sim -N_{nl}/\omega^2$ at large ω), leading to enhanced recombination. The imaginary part of $\alpha_d(\omega)$ always increases recombination. So, a strong maximum in the target photoabsorption cross section results in a similar structure in the RR + PR cross section.

Let us now turn to Pd-like ions with $4d^{10}$ outer subshell. It is well known that photoabsorption by the $4d^{10}$ subshell in atoms and low-charged ions between Pd and Ba is dominated by the $4d \rightarrow \varepsilon f$ giant resonance (see, e.g., [26] and references therein). For example, we have estimated that in Cd^{2+} the $4d$ photoabsorption peaks with $\sigma_{\text{ph}} \approx 23 \text{ Mb}$ at $\omega \approx 60 \text{ eV}$ (cf. neutral Cd [27]). This giant resonance leads to very strong effects in photorecombination. As seen in Fig. 3, in Cd^{2+} and Sn^{4+} PR increases the cross section above the RR background by an order of magnitude for $\omega = 70\text{--}100 \text{ eV}$. As the nuclear charge

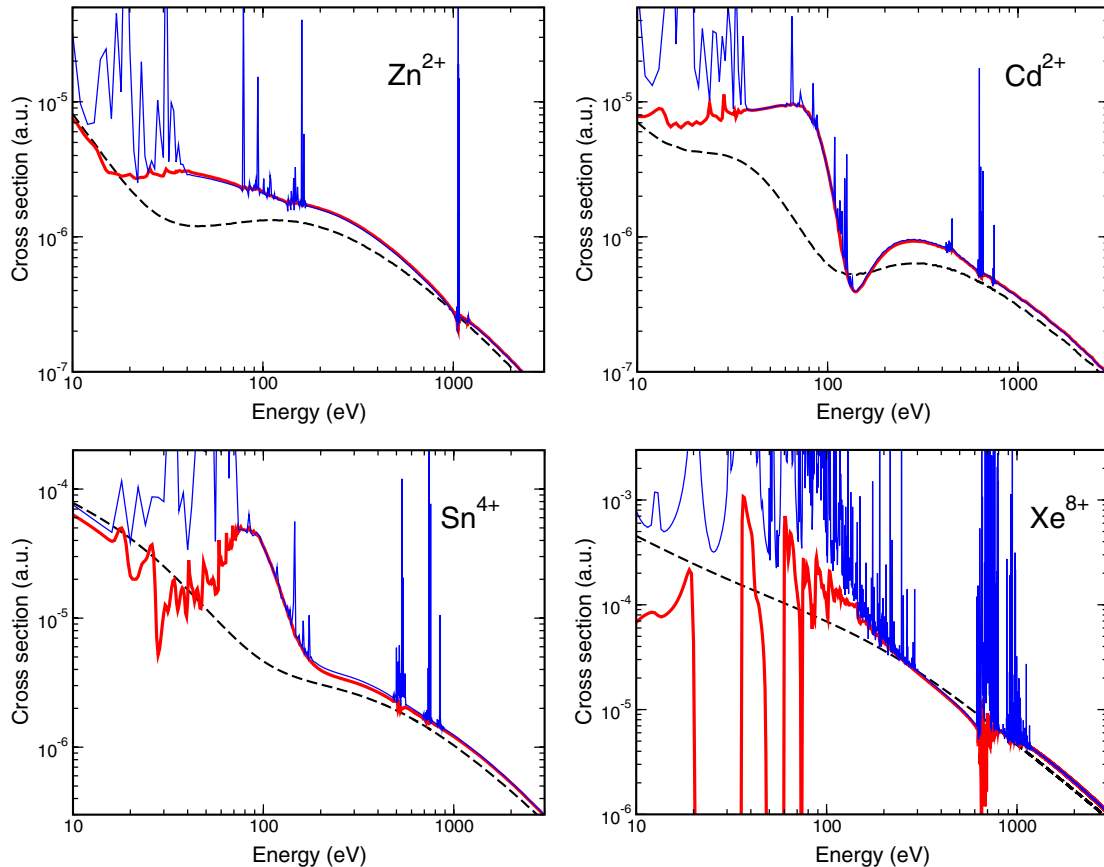


FIG. 3 (color online). Photorecombination cross sections for Zn^{2+} , Cd^{2+} , Sn^{4+} , and Xe^{8+} : RR, dashed curves; RR + PR [Eq. (1)], thin solid curves; RR + PR without resonant contributions, thick solid curves.

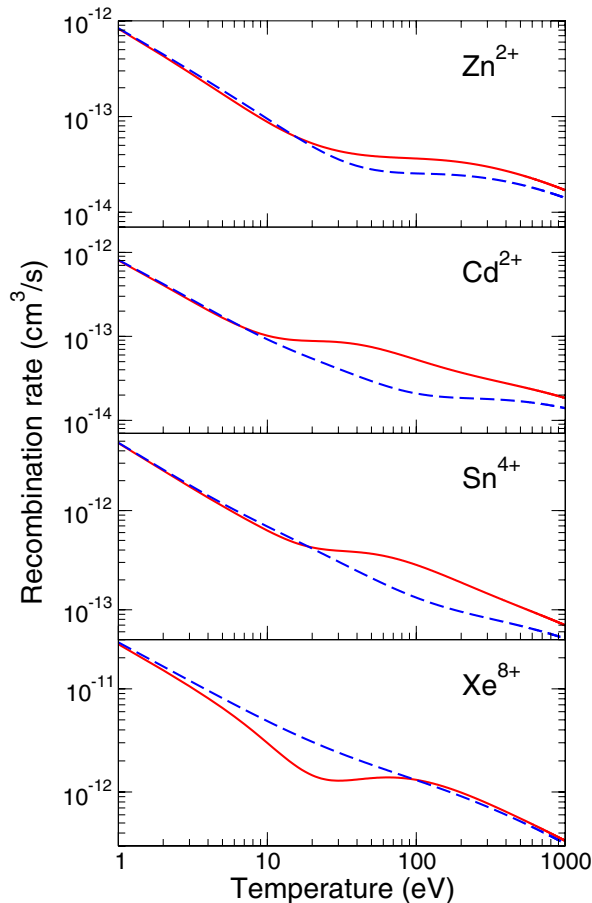


FIG. 4 (color online). Maxwellian recombination rates for Zn^{2+} , Cd^{2+} , Sn^{4+} , and Xe^{8+} obtained from the RR cross sections (dashed curves), and from the RR + PR cross sections (solid curves), omitting any DR resonance contribution.

increases, the $4f$ orbital “collapses”, and the bulk of the dipole strength of the $4d$ subshell is shifted from the giant resonance in the continuum to the $4d \rightarrow nf$ discrete spectrum (see, e.g., [28]). This transition is clear in Fig. 3, when comparing Cd^{2+} , Sn^{4+} , and Xe^{8+} . Simultaneously, the interference between the discrete excitations and the background becomes very large.

For the ions studied in this Letter the PR effects are much larger than for the less polarizable targets examined earlier [20]. Figure 4 shows that they remain important upon thermal averaging, and may thus have a bearing on astrophysical and fusion plasmas, and development of new VUV lithography systems [29].

In summary, we have demonstrated that radiation due to dynamical polarization of the target ion by the incident electron can have a strong influence on the photorecombination cross sections and rates. This effect is strongly enhanced for targets whose photoabsorption cross sections possess giant resonances in the continuum. As such, this important effect may not be accounted for by standard RR + DR calculations.

The authors acknowledge useful discussions with P. G. Burke and the help of R. Kisielius. This work has been

supported by the International Research Centre for Experimental Physics (Queen’s University Belfast).

*Electronic address: korol.rpro@mail.ioffe.ru

†Electronic address: g.gribakin@am.qub.ac.uk

‡Electronic address: f.j.currell@qub.ac.uk

- [1] For ions with complex electronic structure, one may also need to consider “multielectronic” recombination, M. Schnell *et al.*, Phys. Rev. Lett. **91**, 043001 (2003).
- [2] Y. Hahn, Rep. Prog. Phys. **60**, 691 (1997).
- [3] M. Tokman *et al.*, Phys. Rev. A **66**, 012703 (2002).
- [4] S. N. Nahar and A. K. Pradhan, Radiat. Phys. Chem. **70**, 323 (2004).
- [5] M. S. Pindzola, N. R. Badnell, and D. C. Griffin, Phys. Rev. A **46**, 5725 (1992).
- [6] O. Zatsarinny *et al.*, Astron. Astrophys. **412**, 587 (2003).
- [7] T. W. Gorczyca, M. S. Pindzola, F. Robicheaux, and N. R. Badnell, Phys. Rev. A **56**, 4742 (1997).
- [8] T. Mohamed *et al.*, Phys. Rev. A **66**, 022719 (2002).
- [9] E. Behar, V. L. Jacobs, J. Oreg, A. Bar-Shalom, and S. L. Haan, Phys. Rev. A **69**, 022704 (2004).
- [10] S. Schippers *et al.*, Phys. Rev. A **65**, 042723 (2002).
- [11] A. J. González Martínez *et al.*, Phys. Rev. Lett. **94**, 203201 (2005).
- [12] D. M. Mitnik *et al.*, Phys. Rev. A **57**, 4365 (1998).
- [13] A. Hoffknecht *et al.*, J. Phys. B **31**, 2415 (1998).
- [14] G. F. Gribakin, A. A. Gribakina, and V. V. Flambaum, Aust. J. Phys. **52**, 443 (1999).
- [15] V. V. Flambaum, A. A. Gribakina, G. F. Gribakin, and C. Harabati, Phys. Rev. A **66**, 012713 (2002).
- [16] G. F. Gribakin and S. Sahoo, J. Phys. B **36**, 3349 (2003).
- [17] J. Bauche, C. Bauche-Arnoult, and M. Klapisch, *Advances in Atomic and Molecular Physics* (Academic, New York, 1988) Vol. 23, p. 131.
- [18] J.-P. Connerade and A. V. Solov’yov, J. Phys. B **29**, 365 (1996).
- [19] L. Bureeva and V. Lisitsa, J. Phys. B **31**, 1477 (1998); V. A. Astapenko, L. A. Bureeva, and V. S. Lisitsa, Usp. Fiz. Nauk **172**, 155 (2002) [Sov. Phys. Usp. **45**, 149 (2002)].
- [20] A. V. Korol, F. J. Currell, and G. F. Gribakin, J. Phys. B **37**, 2411 (2004).
- [21] M. Ya. Amusia, Phys. Rep. **162**, 249 (1988); A. V. Korol and A. V. Solov’yov, J. Phys. B **30**, 1105 (1997); Radiat. Phys. Chem. **75**, 1266 (2006).
- [22] A. G. Lyalin and A. V. Solov’yov, Radiat. Phys. Chem. **75**, 1358 (2006).
- [23] E. T. Verkhovtseva, E. V. Gnatchenko, A. A. Tkachenko, and B. A. Zon, Radiat. Phys. Chem. **74**, 51 (2005).
- [24] M. S. Pindzola and H. P. Kelly, Phys. Rev. A **14**, 204 (1976).
- [25] A. V. Korol, A. G. Lyalin, and A. V. Solov’yov, J. Phys. B **30**, L115 (1997).
- [26] M. Lysaght *et al.*, Phys. Rev. A **72**, 014502 (2005).
- [27] S. L. Carter and H. P. Kelly, J. Phys. B **11**, 2467 (1978).
- [28] J. M. Bizau *et al.*, Phys. Rev. A **73**, 022718 (2006).
- [29] G. O’Sullivan *et al.*, in *EUV Sources for Lithography*, edited by V. Bakshi SPIE Press Monograph PM149 (SPIE, Washington, 2006), p. 149.